Inorg. Chem. **2006**, *45*, 6922–6927

Structure and Magnetic Properties of a Non-Heme Diiron Complex Singly Bridged by a Hydroxo Group

Josseline Jullien,[†] Gergely Juhász,[§] Pierre Mialane,[†] Eddy Dumas,*[,†] Cédric R. Mayer,[†] Jérôme Marrot,[†] Eric Rivière,[‡] Emile L. Bominaar,*[,§] Eckard Münck,*[,§] and Francis Sécheresse[†]

Institut Lavoisier de Versailles, UMR-CNRS 8180, University of Versailles, 78035 Versailles Cedex, France, Laboratoire de Chimie Inorganique, UMR CNRS 8613, University of Paris-Sud, 91405 Orsay Cedex, France, and Chemistry Department, Carnegie Mellon University, Pittsburgh, Pennsylvania 15213

Received March 9, 2006

The synthesis of the first singly bridged non-heme diiron complex with a μ-hydroxo bridging ligand, [{(salten)Fe}$_2$-(OH)][B(C$_6$H$_5$)$_4$]·(CH$_3$CN)$_x$·(H$_2$O)$_y$ (**1**) [H$_2$salten = 4-azaheptane-1,7-bis(salicylideneiminate)], is reported. The complex has been characterized with X-ray crystallography, FTIR, magnetic susceptibility measurements, and Mössbauer spectroscopy. The data have been compared with the results of DFT calculations on both **1** and a model with an unsupported μ-oxo bridge (**2**) to verify the formulation of the complex as a μ-hydroxo-bridged species. The X-ray structure [Fe–O(H) = 1.997(1) Å and Fe–O(H)–Fe = 159°] is consistent with the DFT-optimized geometry of **1** [Fe–O(H) = 2.02 Å and Fe–O(H)–Fe = 151°]; the Fe–O(H) distance in **1** is about 0.2 Å longer than the Fe–O separations in the optimized geometry of **2** (1.84 Å) and in the crystallographic structures of diiron(III) compounds with unsupported μ-oxo bridges (1.77–1.81 Å). The formulation of **1** as a hydroxo-bridged compound is also supported by the presence of an O–H stretch band in the FTIR spectrum of the complex. The magnetic susceptibility measurements of **1** reveal antiferromagnetic exchange ($J = 42$ cm^{-1} and $H_{ex} = J\mathbf{S}_1\cdot\mathbf{S}_2$). Nearly the same J value is obtained by analyzing the temperature dependence of the Mössbauer spectra ($J = 43$ cm^{-1}; other parameters: $\delta = 0.49$ mm s^{-1}, $\Delta E_Q = -0.97$ mm s^{-1}, and $\eta = 0.45$ at 4.2 K). The experimental J values and Mössbauer parameters agree very well with those obtained from DFT calculations for the μ-hydroxo-bridged compound ($J = 46$ cm^{-1}, $\delta = 0.48$ mm s^{-1}, $\Delta E_Q = -1.09$ mm s^{-1}, and $\eta = 0.35$). The exchange coupling constant in **1** is distinctly different from the value $J \approx 200$ cm^{-1} calculated for the optimized μ-oxo-bridged species, **2**. The increased exchange-coupling in **2** arises primarily from a decrease in the Fe–O bond length.

Introduction

Dinuclear iron complexes with oxo, hydroxo, alkoxo, peroxo, or carboxylato bridge(s) have been extensively studied, mainly because of their relevance as model complexes for metalloenzymes such as methane monooxygenase, ribonucleotide reductase, or intermediates in the catalytic cycles of these metalloenzymes.[1] With dioxygen as an oxidant, diiron complexes have shown significant catalytic activity toward alkane oxidation.[2] While a large number of unsupported μ-oxo-bridged diiron complexes have been structurally characterized,[3] to our knowledge, only four diiron complexes linked by an unsupported μ-hydroxo bridge are known, and those are all porphyrin complexes.[4a−c] Recently,

* To whom correspondence should be addressed. Tel.: 33-1-39-254-383 (E.D.). Fax: 33-1-39-254-381 (E.D.). E-mail: dumas@chimie.uvsq.fr (E.D.), eb7g@andrew.cmu.edu (E.L.B.), emunck@cmu.edu (E.M.).
[†] University of Versailles.
[‡] Université Paris-Sud.
[§] Carnegie Mellon University.

(1) (a) Kurtz, D. M. *Chem. Rev.* **1990**, *90*, 585. (b) Wallar, B. J.; Lipscomb, J. D. *Chem. Rev.* **1996**, *96*, 2625. (c) Solomon, E. I.; Brunold, T. C.; Davis, M. I.; Kemsley, J. N.; Lee, S. K.; Lehnert, N.; Neese, F.; Skulan, A. J.; Yang, Y.-S.; Zhou, J. *Chem. Rev.* **2000**, *100*, 235. (d) Du Bois, J.; Mizoguchi, T. J.; Lippard, S. J. *Coord. Chem. Rev.* **2000**, *200−202*, 443. (e) Tshuva, E. Y.; Lippard, S. J. *Chem. Rev.* **2004**, *104*, 987.
(2) (a) Costas, M.; Chen, K.; Que, L. *Coord. Chem. Rev.* **2000**, *200−202*, 517. (b) Raffard-Pons, Y.; Moll, N.; Banse, F.; Miki, K.; Nierlich, M.; Girerd, J.-J. *Eur. J. Inorg. Chem.* **2002**, 1941.
(3) Eckert, N. A.; Stoian, S.; Smith, J. M.; Bominaar, E. L.; Münck, E.; Holland, P. L. *J. Am. Chem. Soc.* **2005**, *127*, 9344 and references therein. In this paper, Fe−O distances and Fe−O−Fe angles were analyzed in 194 examples (taken from the Cambridge Structural Database) of diiron complexes containing a mono μ-oxo bridge between the two iron centers.

10.1021/ic0604009 CCC: $33.50
Published on Web 07/19/2006

the first example was reported of an unsupported hydroxo bridge linking the non-heme irons of an extended metallo-organic network.[4d] Here, we present the synthesis and characterization of the first non-heme diiron complex with a single μ-hydroxo bridge connecting the iron centers, $[\{(salten)Fe\}_2(OH)][B(C_6H_5)_4]\cdot(CH_3CN)_x\cdot(H_2O)_y$ (**1**) [H_2salten = 4-azaheptane-1,7-bis(salicylideneiminate)]. The experimental structural parameters and exchange-coupling constant for **1** have been compared with those obtained from DFT calculations for this complex and a hypothetical, singly oxo-bridged diiron(III) complex, **2**.

Experimental Section

A. Chemicals and Synthesis of 1. All reagents and solvents were purchased from Aldrich, Acros, or SDS and used as received, without further purification.

A total of 420 μL of salicylaldehyde (4 mmol) and 282 μL of 3,3′-diaminodipropylamine (2 mmol) were mixed together in 50 mL of methanol to give a homogeneous yellow solution A (generating the salten ligand in situ).[5] A total of 810 mg of $Fe(NO_3)_3\cdot 9H_2O$ (2 mmol) was solubilized in 20 mL of methanol and was added to solution A to give a homogeneous dark purple solution. A total of 162 μL of pyridine (2 mmol) was then added (attempts to obtain crystals of **1** without the addition of pyridine remained unsuccessful). The solution was stirred for 1 h, and 2 g of $Na[B(C_6H_5)_4]$ was added. A dark purple precipitate formed after a few hours. The product was isolated by filtration, washed with diethyl ether, and dried at room temperature for a yield of 1.2 g (95%). Recrystallization from acetonitrile afforded X-ray-quality crystals. The amount of acetonitrile (x) and water (y) of crystallization were estimated from an elemental analysis. Anal. Calcd for $C_{68}H_{75}BFe_2N_8O_6$ (with $x = 2$ and $y = 1$): C, 66.79; H, 6.18; B, 0.88; Fe, 9.13; N, 9.16. Found: C, 66.69; H, 6.07; B, 0.94; Fe, 9.39; N, 9.04. The FTIR spectrum of **1** (Figure S1 in the Supporting Information) exhibits a band at 3548 cm^{-1} assigned to the bridging OH stretch and a band at 3225 cm^{-1} attributed to the NH stretching mode.

B. Measurements. The IR spectrum (KBr pellet) was recorded on a FTIR Nicolet Magna-550 spectrophotometer. The UV−vis spectrum (in acetonitrile) was recorded on a Perkin-Elmer Lambda 19 spectrophotometer. X-ray intensity data were collected on a Bruker X8-APEX2 CCD area-detector diffractometer using Mo Kα radiation ($\lambda = 0.710\ 73$ Å). Four sets of narrow data frames (120 s per frame) were collected at different values of θ, for 1 and 3 initial values of ϕ and ω, respectively, using 0.5° increments of ϕ or ω. Data reduction was accomplished using SAINT, v.7.03.21. The substantial redundancy in the data allowed a semiempirical absorption correction (SADABS, v.2.10)[6] to be applied, on the basis of multiple measurements of equivalent reflections. The structure was solved by direct methods, developed by successive difference Fourier syntheses, and refined by full-matrix least-squares on all F^2 data using SHELXTL, v.6.14.[7] Hydrogen atoms (except for H26, which has been located directly from Fourier difference maps) were included in calculated positions and allowed to ride on their parent atoms.

Magnetic susceptibility measurements were carried out with a Quantum Design SQUID magnetometer with an applied field of 0.1 T using powder samples pressed in pellets to avoid preferential orientation of the crystallites by the applied magnetic field. The linearity of the dependence of the magnetization on the applied field was verified at room temperature. The susceptibility data were corrected for diamagnetic contributions by using Pascal's constants and for a monomeric high-spin iron(III) impurity representing 0.9% of the iron content.

Mössbauer spectra were recorded with two spectrometers operating in constant accelerating mode. High-field spectra (8 T) were obtained using Janis Research Super-Varitemp Dewar equipment with a superconducting magnet. Isomeric shifts are quoted relative to the Fe metal at 298 K. Mössbauer spectral simulations were calculated using the WMOSS software package (WEB Research, Edina, MN).

C. Density Functional Calculations. The calculations were performed with Gaussian '03 (revision B.05),[8] using the functional/basis set B3LYP/6-311G. Density functional calculations were carried out on models for complexes **1** and **2**. The geometry optimizations were carried out on models constrained to the observed C_2 symmetry and terminated upon reaching the default convergence criteria. Single-point calculations used tight convergence criteria.

The calculated isomeric shifts (δ) were obtained from the electron density at the ^{57}Fe nucleus using the calibration of Vrajmasu et al.[9] The quadruple splitting (ΔE_Q) and asymmetry parameter (η) were calculated as

$$\Delta E_Q = \frac{1}{2} eQV_{zz}\sqrt{1+\frac{1}{3}\eta^2} \tag{1}$$

and

$$\eta = \frac{V_{xx} - V_{yy}}{V_{zz}} \tag{2}$$

where Q is the nuclear quadrupole moment of ^{57}Fe and V_{ii} ($i = x$, y, and z) are the principal components of the electric field gradient (EFG) tensor at the Fe nucleus calculated using the Property keyword of Gaussian '03. The calculated ΔE_Q values are based on $Q = 0.17$ barn, which implies the factor of -1.7 mm s^{-1}/au for converting the Gaussian output for the EFG (given in atomic units) to mm s^{-1}.

(4) (a) Scheidt, W. R.; Cheng, B.; Safo, M. K.; Cukiernik, F.; Marchon, J.-C.; Debrunner, P. G. *J. Am. Chem. Soc.* **1992**, *114*, 4420. (b) Evans, D. R.; Mathur, R. S.; Heerwegh, K.; Reed, C. A.; Xie, Z. *Angew. Chem., Int. Ed. Engl.* **1997**, *36*, 1335. (c) Hung, C.-H.; Chen, W.-C.; Lee, G.-H.; Peng, S.-M. *Chem. Commun.* **2002**, 1516. (d) Armentano, D.; De Munno, G.; Mastropietro, T. F.; Julve, M.; Lloret, F. *J. Am. Chem. Soc.* **2005**, *127*, 10778.

(5) Matsumoto, N.; Ohta, S.; Yoshimura, C.; Ohyoshi, A.; Kohata, S.; Okawa, H.; Maeda, Y. *J. Chem. Soc., Dalton Trans.* **1985**, 2575.

(6) *APEX2*, version 1.0-8; Bruker AXS: Madison, WI, 2003.

(7) *SHELXTL*, version 6.14; Bruker AXS: Madison, WI, 2001.

(8) Frisch, M. J.; Trucks, G. W.; Schlegel, H. B.; Scuseria, G. E.; Robb, M. A.; Cheeseman, J. R.; Montgomery, J. A.; Vreven, T., Jr.; Kudin, K. N.; Burant, J. C.; Millam, J. M.; Iyengar, S. S.; Tomasi, J.; Barone, V.; Mennucci, B.; Cossi, M.; Scalmani, G.; Rega, N.; Petersson, G. A.; Nakatsuji, H.; Hada, M.; Ehara, M.; Toyota, K.; Fukuda, R.; Hasegawa, J.; Ishida, M.; Nakajima, T.; Honda, Y.; Kitao, O.; Nakai, H.; Klene, M.; Li, X.; Knox, J. E.; Hratchian, H. P.; Cross, J. B.; Adamo, C.; Jaramillo, J.; Gomperts, R.; Stratmann, R. E.; Yazyev, O.; Austin, A. J.; Cammi, R.; Pomelli, C.; Ochterski, J. W.; Ayala, P. Y.; Morokuma, K.; Voth, G. A.; Salvador, P.; Dannenberg, J. J.; Zakrzewski, V. G.; Dapprich, S.; Daniels, A. D.; Strain, M. C.; Farkas, O.; Malick, D. K.; Rabuck, A. D.; Raghavachari, K.; Foresman, J. B.; Ortiz, J. V.; Cui, Q.; Baboul, A. G.; Clifford, S.; Cioslowski, J.; Stefanov, B. B.; Liu, G.; Liashenko, A.; Piskorz, P.; Komaromi, I.; Martin, R. L.; Fox, D. J.; Keith, T.; Al-Laham, M. A.; Peng, C. Y.; Nanayakkara, A.; Challacombe, M.; Gill, P. M. W. B.; Johnson, W. Chen, Wong, M. W.; Gonzalez, C.; Pople, J. A. *Gaussian 03*, revision B.05; Gaussian, Inc.: Pittsburgh, PA, 2003.

(9) Vrajmasu, V.; Münck, E.; Bominaar, E. *Inorg. Chem.* **2003**, *42*, 5974.

Table 1. Crystal Data and Structure Refinement for Complex **1**

	1
empirical formula	$C_{68}H_{75}BFe_2N_8O_6$
formula wt, g	1222.90
cryst syst	orthorhombic
space group	P*ccn*
a, Å	18.6426(7)
b, Å	17.6990(7)
c, Å	18.6234(7)
α, deg	90
β, deg	90
γ, deg	90
V, Å^3	6144.9(4)
Z	4
ρ_{calcd}, g cm^{-3}	1.300
T, K	293(2)
rflns unique/rfns obsd	34220/8072
R_{int}	0.0490
R [$>2\sigma(I)$]	$R_1(F_o)^a = 0.0468$ $wR_2(F_o^2)^b = 0.1157$
R (all data)	$R_1(F_o)^a = 0.1042$ $wR_2(F_o^2)^b = 0.1386$

$^a R_1 = \sqrt{\sum||F_o|-|F_c||/\sum|F_c|}$ $^b wR_2 = \sqrt{\sum w(F_o^2-F_c^2)^2/\sum w(F_o^2)^2}$

The exchange-coupling constant was calculated with the broken-symmetry (BS) method,[3,10] using the expression $J = [E(\mathrm{F}) - E(\mathrm{BS})]/12.5$ (convention: $J\mathbf{S}_1\cdot\mathbf{S}_2$) where E(F) and E(BS) are the total self-consistent field energies of the ferromagnetic (F) and BS states, respectively.

Results and Discussion

Stucture of Complex 1. Complex **1** crystallizes in the orthorhombic space group *Pccn* (Table 1). Figure 1 shows the X-ray structure of the cation $[\{(\mathrm{salten})\mathrm{Fe}\}_2(\mathrm{OH})]^+$. The two $\{\mathrm{Fe(salten)}\}^+$ units of the dimetallic cation are crystallographically equivalent. The Fe atoms reside in a distorted octahedral environment comprising three nitrogen and two oxygen atoms of a salten ligand and the hydroxo bridge. The distances and angles in the salten ligand are comparable with the ones previously reported in compounds containing the {Fe(salten)} unit.[5,11] The Fe−O_{salten}, Fe−N_{amino}, and Fe−N_{imido} distances are in the range expected for a high-spin Fe^{III} center.[12] The Fe−O(H) distance of 1.997(1) Å is larger than the Fe−O(H) distance observed in unsupported *μ*-hydroxo-bridged porphyrin diiron complexes [1.821(8) − 1.984(3) Å],[4] but well within the range of the Fe−O(H) distances in $Fe^{III}_2(\mu\text{-OH})_2$ complexes (1.937−2.092 Å),[13] and much longer than the Fe−O distances in unsupported *μ*-oxo-bridged diiron complexes (average 1.774 Å, standard dev. 0.029 Å).[3] The nature of the bridge is confirmed by IR spectroscopy [ν(OH) = 3548 cm^{-1}] and valence bond summations (VBS) ($VBS_{O(26)} = 1.05$).[14]

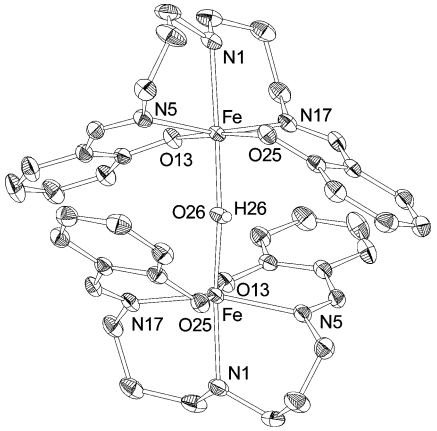

Figure 1. Molecular structure of $[\{(\mathrm{salten})\mathrm{Fe}\}_2(\mathrm{OH})]^+$ (30% thermal ellipsoid probability). Hydrogen atoms of the two salten ligands are omitted for clarity. Selected bond distances (Å) and angles (deg): Fe−O(13) 1.917(2), Fe−O(25) 1.971(2), Fe−O(26) 1.997(1), Fe−N(1) 2.255(2), Fe−N(5) 2.148(2), Fe−N(17) 2.082(2), Fe−Fe 3.928(1), Fe−O(26)−Fe 159.45(14).

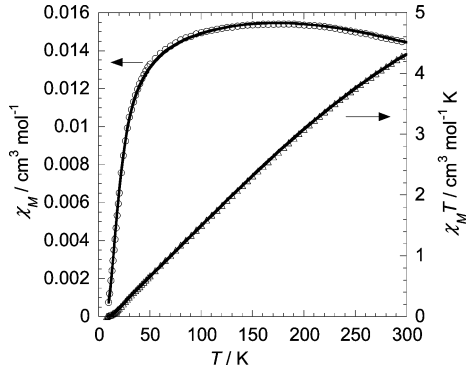

Figure 2. $\chi_M T$ versus T (△) and χ_M versus T (○) for **1**. The solid lines are the best fits using the values given in the text.

Magnetic Properties and Mössbauer Spectroscopy. The magnetic properties of three of the four previously reported unsupported *μ*-hydroxo-bridged porphyrin diiron complexes have been studied; however, in $\{[\mathrm{Fe(OEP)}]_2(\mathrm{OH})\}^+$ (OEP = octaethylporphyrinate), the presence of impurities prevented an accurate determination of the exchange-coupling constant J,[4a] and in $\{[\mathrm{Fe(TPP)}]_2(\mathrm{OH})\}^{1+}$ (TTP = tetraphenylporphyrinate), surprisingly, vanishing ($|J| < 3$ cm^{-1}) exchange interactions were found for both the $[CB_{11}H_6Cl_6]^-$ and $[F_{20}-BPh_4]^-$ isolated complexes.[4b] For the compounds of refs 4c and d, no values for J were reported.

Figure 2 shows the magnetic behavior of polycrystalline **1**. $\chi_M T$ decreases upon cooling from $\chi_M T = 4.33$ cm^3 mol^{-1} K at 300 K to a value of 0.03 cm^3 mol^{-1} K at 4.2 K, indicating an antiferromagnetically coupled system with a

(10) (a) Noodleman, L.; Baerends, E. J. *J. Am. Chem. Soc.* **1984**, *106*, 2316. (b) Noodleman, L. *J. Chem. Phys.* **1981**, *74*, 5737.
(11) (a) Wang, X.; Kotun, M. E.; Pennington, W. T.; Fanning, J. C. *Inorg. Chim. Acta* **1988**, *154*, 189. (b) Hayami, S.; Inoue, K.; Osaki, S.; Maeda, Y. *Chem. Lett.* **1998**, 987. (c) Hirose, S.; Hayami, S.; Maeda, Y. *Bull. Chem. Soc. Jpn.* **2000**, *73*, 2059. (d) Hayami, S.; Hosokoshi, Y.; Inoue, K.; Einaga, Y.; Sato, O.; Maeda, Y. *Bull. Chem. Soc. Jpn.* **2001**, *74*, 2361. (e) Park, S.-M.; Kim, Y.; Kim, S.-J. *Eur. J. Inorg. Chem.* **2003**, 4117.
(12) Floquet, S.; Carmen Muñoz, M.; Rivière, E.; Clément, R.; Audière, J.-P.; Boillot, M.-L. *New J. Chem.* **2004**, *28*, 535.
(13) (a) Nanda, K. K.; Dutta, S. K.; Baitalik, S.; Venkatsubramanian, K.; Nag, K. *J. Chem. Soc., Dalton Trans.* **1995**, *7*, 1239. (b) Burger, J.; Klüfers, P. *Z. Anorg. Allg. Chem.* **1996**, *622*, 1740. (c) Dutta, S. K.; Nanda, K. K.; Flörke, U.; Bhadbhade, M.; Nag, K. *J. Chem. Soc., Dalton Trans.* **1996**, *11*, 2371. (d) Kurosaki, H.; Yoshida, H.; Ito, M.; Koike, H.; Higuchi, E.; Goto, M. *Bioorg. Med. Chem. Lett.* **2001**, *11*, 785 and references therein. (e) Zhu, S.; Brennessel, W. W.; Harrison, R. G.; Que, L., Jr. *Inorg. Chim. Acta* **2002**, *337*, 32. (f) Tanase, S.; Bouwman, E.; Long, G. J.; Shahin, A. M.; Mills, A. M.; Spek, A. L.; Reedijk, J. *Eur. J. Inorg. Chem.* **2004**, 4572.
(14) Brese, N. E.; O'Keeffe, M. *Acta Crystallogr., Sect. B* **1991**, *47*, 192.

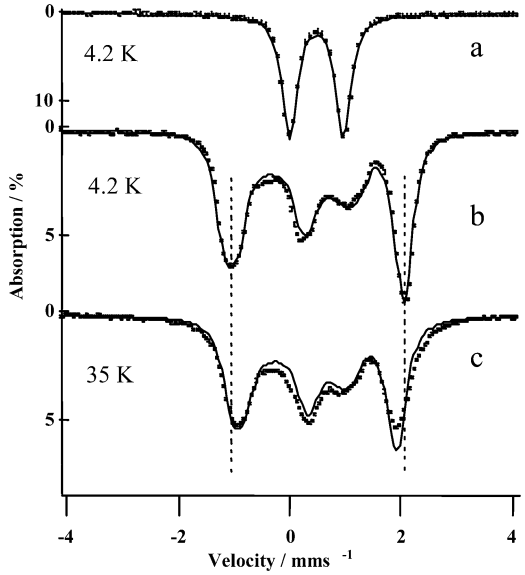

Figure 3. Mössbauer spectra of polycrystalline **1** recorded in a zero magnetic field (a) and 8.0 T magnetic fields (b and c) applied parallel to the γ radiation, at the temperatures indicated. Solid lines are spectral simulations based on eqs 3−5, using $\Delta E_Q = -0.97$ mm s^{-1}, $\eta = 0.45$, $A = -28$ MHz, and $J = 43$ cm^{-1}. The dotted lines show the effect of the temperature on B_{int}.

diamagnetic ground state. The χ_M versus T curve was simulated using the spin Hamiltonian

$$H_e = J\mathbf{S}_1\cdot\mathbf{S}_2 + g_1\beta\mathbf{S}_1\cdot\mathbf{B} + g_2\beta\mathbf{S}_2\cdot\mathbf{B} \quad (3)$$

where $S_1 = S_2 = {}^5/_2$ are the spins of the two high-spin ferric ions and $g_1 = g_2 = 2.00$. Equation 3 does not include terms for zero-field splitting because these interactions are small in non-heme high-spin ferric sites and only split the excited, $S > 0$ spin multiplets of the coupled system. As a result, the powder-averaged susceptibility data and the Mössbauer spectra are quite insensitive to these quantities. The best fit to the χ_M versus T curve yielded $J = 41.8 \pm 0.4$ cm^{-1}. The $\chi_M T$ versus T curve can be fitted considering the same J value (Figure 2). Such a J value is much smaller than those for unsupported oxo-bridged diiron(III) species, which have $180 < J < 230$ cm^{-1},[15] larger than those reported for bis(μ-OH) species ($5.6 < J < 22.0$ cm^{-1}),[1c,13f] and similar to those reported for carboxylato-supported hydroxo-bridged species, supporting the notion that superexchange in this class of molecules is dominated by interactions between the metal centers and the hydroxo bridge.[16]

Figure 3a shows a 4.2 K Mössbauer spectrum of polycrystalline **1** recorded in the absence of an applied magnetic field. It consists of a single quadrupole doublet with $|\Delta E_Q| = 0.97(2)$ mm s^{-1} and $\delta = 0.48(1)$ mm s^{-1}. The observation of one doublet is consistent with the X-ray structure, which has revealed structurally equivalent sites. The isomer shift is typical for high-spin ferric sites with octahedral N/O coordination. It has been shown that Mössbauer spectroscopy can be used to measure the exchange-coupling constant for antiferromagnetically coupled $Fe^{III}Fe^{III}$ dimers, provided $J \leq 100$ cm^{-1}.[17] Thus, complex **1** gives the opportunity to determine J with different techniques. Figure 3b shows an 8.0 T spectrum of **1** recorded at 4.2 K; the solid line is a theoretical spectrum generated under the assumption that only the $S = 0$ ground state is measurably populated at this temperature. We have also recorded 8.0 T spectra at 15, 22, 35 (Figure 3c), and 60 K. It can be seen that the magnetic splitting at 35 K is smaller than that at 4.2 K. The decrease can be attributed to population of the $S = 1$ manifold, which is the first excited state in the spin ladder of the coupled system. If relaxation between the $S = 0$ ground state and the $S = 1$ levels ($M_S = \pm 1, 0$) were slow, we would have observed four Mössbauer spectra at 35 K, each of them associated with one of the four magnetic sublevels and weighted with the appropriate Boltzmann factor. In the fast relaxation limit, the situation encountered for **1**, only one spectrum is observed, for which the effective magnetic fields at the Fe nuclei are given by

$$\mathbf{B}_{eff}(i) = \mathbf{B} - \langle\mathbf{S}_i\rangle_T A(i)/g_n\beta_n \quad (4)$$

where $i = 1$ and 2 labels the Fe sites.[18] The thermally averaged expectation value $\langle\mathbf{S}_i\rangle_T$ depends on the energy separation, J, between the $S = 0$ ground state and the $S = 1$ excited-state manifold. By fitting the temperature dependence of $\langle\mathbf{S}_i\rangle_T$, the exchange parameter J has been determined. For our simulations, we have used the Hamiltonian of eq 5 to describe the hyperfine interactions of the ^{57}Fe nucleus.

$$H = H_e + H_n(1) + H_n(2) \quad (5)$$

$$H_n(i) = -g_n\beta_n\mathbf{B}\cdot\mathbf{I}_i + \mathbf{S}_i\cdot\mathbf{A}_i\cdot\mathbf{I}_i + H_Q(i) \quad (6)$$

In eq 6, $H_Q(i)$ describes the quadrupole interaction, and because the iron sites are high-spin ferric, we have assumed isotropic magnetic hyperfine interactions, $A_i = -29$ MHz. The best simulations to the Mössbauer spectra were obtained for $J = 43$ cm^{-1}, in excellent agreement with the magnetic data; by visual comparison of spectral simulations, we estimate for J an uncertainty of ± 3 cm^{-1}.

DFT Analysis. The results of the DFT calculations for $\{[Fe(salten)]_2(OH)\}^{1+}$ are in excellent agreement with the experimental data (given in parentheses): Fe−O(H) = 2.02 (2.00) Å, Fe−O(H)−Fe = 151° (159°), $\delta = 0.48$ (0.48) mm s^{-1}, $\Delta E_Q = -1.09$ (−0.97) mm s^{-1}, $\eta = 0.35$ (0.45), and J

(15) Wasser, I. M.; Martens, C. F.; Verani, C. N.; Rentschler, E.; Huang, H.-W.; Moënne-Loccoz, P.; Zakharov, L. N.; Rheingold, A. L.; Karlin, K. D. *Inorg. Chem.* **2004**, *43*, 651.
(16) Weldon, B. T.; Wheeler, D. E.; Kirby, J. P.; McCusker, J. K. *Inorg. Chem.* **2001**, *40*, 6802.
(17) (a) Kauffmann, K. E.; Münck, E. *Spectroscopic Methods in Bioinorganic Chemistry*; ACS Symposium Series 692; American Chemical Society: Washington, DC, 1998. (b) Zang, Y.; Dong, Y. L.; Que, L., Jr.; Kauffmann, K.; Münck, E. *J. Am. Chem. Soc.* **1995**, *117*, 1169. (c) Krebs, C.; Bollinger, J. M.; Theil, E. C.; Huynh, B. H. *J. Biol. Inorg. Chem.* **2002**, *7*, 863.
(18) At 35 K, the lines are slightly broader than at 4.2 K, suggesting that the electronic system is not strictly in the fast fluctuation limit at 35 K. At 4.2 K, the relaxation rate is probably slow, but because only the $S = 0$ state is significantly populated at 4.2 K, the Mössbauer spectrum is independent of the relaxation rate.

= 46 (42 and 43) cm^{-1}.[19] To further explore the effect of the hydroxo bridge on the electronic structure of **1**, we have also performed DFT calculations for the hypothetical, deprotonated complex $[Fe(salten)]_2O$ (**2**). The calculations for **2** yield Fe−O = 1.81 Å, Fe−O−Fe = 177°, δ = 0.48 mm s^{-1}, ΔE_Q = −1.22 mm s^{-1}, η = 0.70, and J = 203 cm^{-1}.[19] It is noteworthy that the calculations predict an almost linear Fe−O−Fe unit, a substantially shorter Fe−O distance, and a considerably larger value for J. Hence, the DFT calculations strongly support the formulation of **1** as a hydroxo-bridged species, a conclusion that is also consistent with the charge of complex **1** deduced from the crystal structure. The DFT values for Fe−O[20] and J in **2** are consistent with the Fe−O distances (1.77−1.81 Å) and coupling constants ($J \approx 200$ cm^{-1}) obtained from magnetic susceptibility studies of unsupported oxo-bridged diiron(III) complexes.[1a]

To identify the structural factor(s) responsible for the large influence that deprotonation of the hydroxo bridge has on the exchange coupling, we have compared the J values calculated in a series of geometries that represent a step-by-step transition from the optimized geometry of **1** (**1a**) to the optimized geometry of **2** (**2d**);[21] details are given in Tables S1 and S2 of the Supporting Information. First, deprotonation of the μ-hydroxo bridge of **1** yields a μ-oxo-bridged structure **2a** (i.e., deprotonated **1a**) for which the bond distances and angles are kept identical to those of **1a**. The calculated J value for **2a** is J_{2a} = 70 cm^{-1}, which is moderately higher than J_{1a} = 46 cm^{-1}. Second, increasing the Fe−O−Fe angle of **2a** from 150° to 177° yields structure **2b** with a J_{2b} (= 59 cm^{-1}) that is only slightly smaller than J_{2a}. Third, by decreasing the Fe−O bond length in **2b** to 1.84 Å, we obtain structure **2c** that has an Fe−O−Fe unit identical to the one in the structure optimized in the ferromagnetic state, **2d**, and the Fe-salten coordination of **1a**. The calculated J_{2c} = 181 cm^{-1} is close to J_{2d} = 186 cm^{-1}.[21] The preceding analysis indicates that the increase in J is primarily due to a shortening of the Fe−O distance, while other factors, such as the Fe−O−Fe bond angle and the hydroxo proton, play only a secondary role. Gorun and Lippard have deduced a similar correlation between J and the Fe−O distance from the magneto-structural data for the large class of diiron(III) complexes with *supported* oxo bridges.[22] In this class, J increases from ∼20 cm^{-1} at 2.08 Å to ∼240 cm^{-1} at 1.76 Å. The Fe−O(H) distance and J value for **1** are similar to those for the diacetato, hydroxo-bridged diiron(III) complex $[Fe(HB(pz)_3]_2(OH)(OAc)_2$ [Fe−O(H) = 1.95 Å and J = 35 cm^{-1}],[23] supporting the notion that the exchange interaction is primarily mediated by the hydroxo bridge. There are also theoretical studies investigating the correlation between the structural parameters and J in μ-oxo and μ-hydroxo-bridged compounds. Hart et al.[24] reported a strong distance dependence and a weak angular dependence of exchange interaction in the unsupported bridged μ-oxo compound, $[Fe_2OCl_6]^{2-}$. The theoretical calculations of Chen et al.[25] showed that the protonation of the bridging oxygen of $[Fe_2OCl_6]^{2-}$ results in a weakening of exchange interactions and a significantly lower J.

To date, the only unsupported hydroxo-bridged diiron(III) species available for comparison with **1** are the binuclear porphyrin complexes $\{[Fe(OEP)]_2(OH)\}^{1+}$ and $\{[Fe(TPP)]_2(OH)\}^{1+}$.[4a,b] The magneto-structural data for these compounds are Fe−O(H)OEP = 1.94 Å and 100 $cm^{-1} < J_{OEP} <$ 320 cm^{-1} for the OEP complex[26] and $Fe-O(H)_{TPP}$ = 1.87 Å[27] and $|J_{TPP}| < 3$ cm^{-1} for the TPP complex. The data for the OEP complex and **1** satisfy the inequalities $Fe-O(H)_{OEP} < Fe-O(H)_1$[28] and $J_{OEP} > J_1$ and fulfill the proposed correlation between J and the Fe−O distance. However, the TPP complex, despite having a shorter Fe−O(H) distance [$Fe-O(H)_{TPP} < Fe-O(H)_1$ and $Fe-O(H)_{OEP}$], has a vanishing exchange coupling ($J_{TPP} \ll J_1$ and J_{OEP}).[29] Studies of the TPP complex along the lines described here may provide new insights into this unusual behavior.

Conclusion

In summary, the first non-heme dinuclear iron(III) complex with an unsupported hydroxo bridge has been synthesized and structurally and magnetically characterized. The value for J has been determined from independent analyses of magnetic susceptibility data and Mössbauer spectra (40 $cm^{-1} < J <$ 45.0 cm^{-1} and $H = J\mathbf{S}_1\cdot\mathbf{S}_2$). The J value is in excellent agreement with the DFT result (J = 46 cm^{-1}) and is considerably smaller than the couplings reported for diiron(III)

(19) The J was obtained with the expression $J = (E_F - E_{BS})/12.5$, using the DFT total energies for the ferromagnetic state (E_F) and the broken symmetry state (E_{BS}) that were evaluated at the optimized geometries for the F state and BS state, respectively. The other parameters were calculated for the BS state at the optimized BS geometry. A detailed account of the calculations is given in the Supporting Information.

(20) The DFT calculations yield Fe−O distances that are ∼0.02 Å longer than those obtained from X-ray analysis, cf. Table 1. Correcting the calculated Fe−O distance (1.81 Å) accordingly yields 1.79 Å, which is in the middle of the experimental range.

(21) For reasons of computational convenience, we adopted for this analysis the optimized structures for the ferromagnetic (S = 5) state, **1a** and **2d**. The Fe−O distances in **1a** (2.03 Å) and **2d** (1.84 Å) are slightly longer than those in the optimized structures for the BS states (2.02 and 1.81 Å, respectively). The value J_{2d} = 186 cm^{-1} was obtained with the expression given in ref 19 and values for E_F and E_{BS} that were both evaluated at the optimized geometry for the F state. The J value (186 cm^{-1}) is slightly smaller than the value given in ref 19 (203 cm^{-1}) because the E_{BS} value adopted here is the energy for a structure that is not fully relaxed in the BS state.

(22) Gorun, S. M.; Lippard, S. J. *Inorg. Chem.* **1991**, *30*, 1625.

(23) Armstrong, W. H.; Lippard, S. J. *J. Am. Chem. Soc.* **1984**, *106*, 4632.

(24) Hart, J. R.; Rappé, A. K.; Gorun, S. M.; Upton, T. H. *Inorg. Chem.* **1992**, *31*, 5254.

(25) Chen, Z.; Xu, Z.; Zhang, L.; Yan, F.; Lin, Z. *J. Phys. Chem. A* **2001**, *105*, 9710.

(26) J has not been accurately determined because of the presence of paramagnetic impurities, cf. ref 4a.

(27) The value 1.87 Å is the average over the distances in two crystalline forms, $(Fe-O)_A$ = 1.92 Å and $(Fe-O)_B$ = 1.82 Å.

(28) A plausible explanation for the shorter Fe−O distance in the porphyrin species is that the iron therein is 5-coordinate, allowing it to move out of the pyrrole nitrogen plane.

(29) The two porphyrin complexes contain iron sites with spin-admixed, $S = {}^5/_2$ and ${}^3/_2$ ground states. The $S = {}^3/_2$ configuration results from the $3d^5$, $S = {}^5/_2$ configuration by the spin-flip transition $(x^2 - y^2)^\alpha \rightarrow (xy)^\beta$ (x and y axes are directed along the Fe−N vectors). Because the overlaps between the latter orbitals and those of the bridging ligand are small, the admixture of the $S = {}^3/_2$ configuration should have little effect on the exchange splittings.

complexes with an unsupported oxo bridge ($J \approx 200$ cm^{-1}). DFT calculations show that lengthening of the Fe−O−Fe bonds, caused by protonation of the oxo bridge, is the major determinant for the decrease of J.

Acknowledgment. We thank the National Institutes of Health for support of this research under EB001475 (E.M.) and Dr. S. Floquet for fruitful discussions during the preparation of this manuscript.

Supporting Information Available: Absorption and IR spectra, DFT calculation tables, and an X-ray crystallographic file in CIF format. This material is available free of charge via the Internet at http://pubs.acs.org.

IC0604009